WORLD METEOROLOGICAL ORGANIZATION

GLOBAL ATMOSPHERE WATCH

No. 1 – SEPTEMBER 2021

WMO AIR QUALITY AND CLIMATE BULLETIN

Introduction

Ongoing climate change, caused by the accumulation of greenhouse gases in the atmosphere, is happening on a timescale of decades to centuries and is driving environmental changes worldwide. In contrast, the impacts of air pollution occur near the surface, on timescales of days to weeks, and across spatial scales that range from local (for example, urban centres, see the photo below) to regional. Despite these wide-ranging differences, air quality and climate change are strongly interconnected (Fiore et al., 2012; West et al., 2013; IPCC, 2021). The new *WMO Air Quality and Climate Bulletin* will report annually on the state of air quality and its connections to climate change, reflecting on the geographical distribution of and changes in traditional pollutants.

Traditional pollutants include short-lived reactive gases such as ozone – a trace gas that is both a common air pollutant and a greenhouse gas that warms the atmosphere – and particulate matter – a wide range of tiny particles suspended in the atmosphere (commonly referred to as aerosols), which are detrimental to human health and whose complex characteristics can either cool or warm the atmosphere.

Air quality and climate are interconnected because the chemical species that affect both are linked, and because changes in one inevitably cause changes in the other. Human activities that release long-lived greenhouse gases into the atmosphere also enhance the concentrations of shorter-lived ozone and particulate matter in the atmosphere. For example, the combustion of fossil fuels (a major source of carbon dioxide (CO_2)) also emits nitrogen oxide (NO) into the atmosphere, which can lead to the photochemical formation[1] of ozone and nitrate aerosols. Similarly, agricultural activities (which are major sources of the greenhouse gas methane) emit ammonia, which then forms ammonium aerosols (Pye et al., 2009).

Policy changes that seek to improve air quality thus have repercussions on those policies that seek to limit climate change, and vice versa. For instance, a drastic reduction in fossil fuel combustion to reduce greenhouse gas emissions will also reduce air pollutants associated with that activity, such as ozone and nitrate aerosols. Policies to reduce particulate matter pollution to protect human health may remove the cooling effect of sulfate aerosols or the warming effect of black carbon (soot particles). Finally, changes in climate can influence pollution levels directly. For example, the increased frequency and intensity of heatwaves may lead to the additional accumulation of pollutants close to the surface.

Combo shows the India Gate war memorial on October 17, 2019 (top) and after air pollution levels started to drop during a 21-day nationwide lockdown in New Delhi, India, April 8, 2020 (bottom). Improvement in air quality can be driven by many processes, including emission reduction and changes in meteorological conditions as explained in this Bulletin. *Source*: Reuters/Anushree Fadnavis/Adnan Abidi

[1] Photochemical formation is a chemical reaction in which a molecule is formed in the presence of light.

This issue of the *WMO Air Quality and Climate Bulletin* provides an update on the current global distribution of particulate matter, highlighting the contributions of extreme wildfire events in the year 2020. 2020 was also notable for the spread of a new coronavirus (SARS-CoV-2), which causes the respiratory illness known as COVID-19. The ensuing COVID-19 pandemic triggered a worldwide economic downturn in 2020, which led to reduction of the emissions of air pollutants, yielding a range of impacts on surface and free tropospheric[2] levels of ozone and particulate matter (Gkatzelis et al., 2021; Steinbrecht et al., 2021). This Bulletin reviews many new and important scientific findings on the impact of COVID-19 on air quality around the world, based on long-term measurements taken at certain WMO Global Atmosphere Watch (GAW) stations. It ends with a recent update on the global health impact of long-term exposure to ozone and particulate matter pollution.

Global particulate matter concentrations in 2020 recorded by the Copernicus Atmosphere Monitoring Service

Inhaling particulate matter smaller than 2.5 micrometres ($PM_{2.5}$) over long periods is a severe health hazard. Human and natural sources contribute to $PM_{2.5}$ pollution in varying proportions at the global scale. Using the $PM_{2.5}$ data from the Copernicus Atmosphere Monitoring Service (CAMS) re-analysis, Figure 1 shows the average $PM_{2.5}$ surface concentrations for 2003–2019 and the anomalies (absolute differences) in 2020 compared with the mean values for 2003–2019.

Intense wildfires generated anomalously high $PM_{2.5}$ concentrations in several parts of the world that were unusually dry and hot in 2020. In January and the preceding December, southwestern Australia was affected by widespread wildfires, which exacerbated air pollution (see also *WMO Aerosol Bulletin 2021*). Smoke from the Australian fires also led to temporary cooling across the southern hemisphere, comparable to that caused by ash from a volcanic eruption (Fasullo et al., 2021). Enhanced wildfire activity also occurred in the Yakutia region of Siberia, in the US state of California and many other regions of the western United States of America. Regularly occurring wildfires in central South America and central Africa were also higher than the 2003–2019 average. The lower-than-average $PM_{2.5}$ concentrations over western Canada, Indonesia and northern Australia were caused by below-average wildfire activity in the respective regions.

The variability of $PM_{2.5}$ due to desert dust is evident above large desert areas and the adjacent outflow regions. While the eastern Sahara had lower surface $PM_{2.5}$ concentrations than usual, more frequent dust transport events, including the exceptionally strong *Godzilla* dust storm in June 2020, led to increased $PM_{2.5}$ over the North Atlantic Ocean (Chakraborty et al., 2021). Weaker-than-usual dust emissions also occurred in the desert regions of northern China and Mongolia. For details, please refer to the *WMO Airborne Dust Bulletin*.

Aerosols originating from human activity have the largest impact on human health because they contribute most to $PM_{2.5}$ in highly populated areas. In 2020, there was an unprecedented reduction in certain human activities, such as vehicle transport and aviation, due to the economic downturn associated with the COVID-19 pandemic. In areas such as China, Europe and North America, short-term COVID-related reductions in emissions coincided with long-term emission-mitigation measures that led to lower $PM_{2.5}$ concentrations in 2020 compared to previous years. The increase in $PM_{2.5}$ over India was less pronounced than in previous years. A better understanding of the multiple natural and anthropogenic sources of emissions and the meteorological influences on emissions and on the spread of the resulting pollution are critical for advancing our modelling of atmospheric composition and its changes.

CAMS methodology

Combining computer models with near-real-time observations – a process known as data assimilation – has been

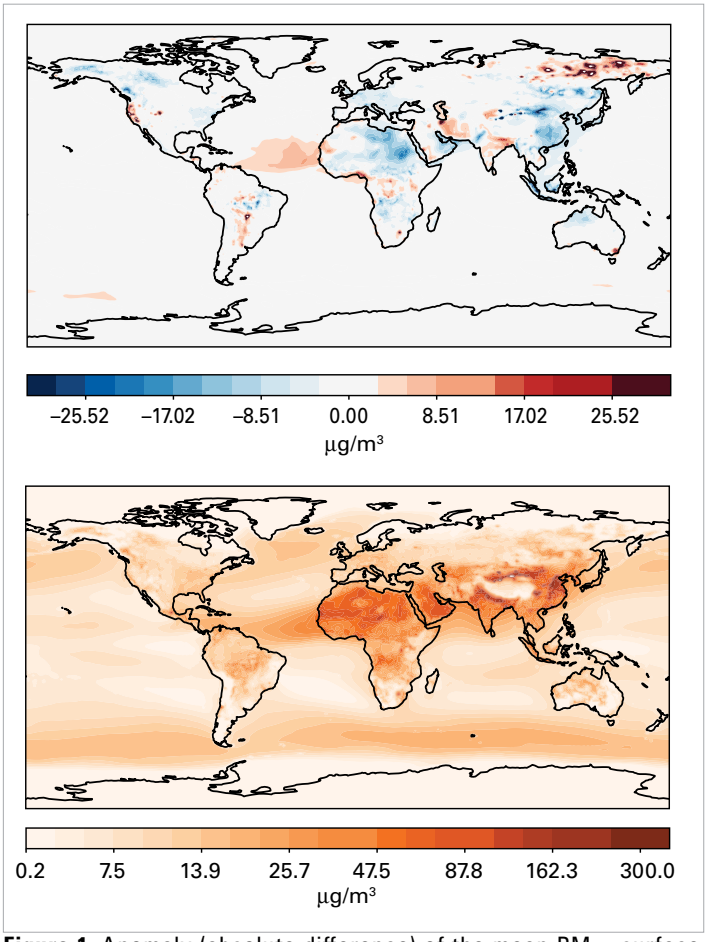

Figure 1. Anomaly (absolute difference) of the mean $PM_{2.5}$ surface concentrations (µg/m³) in 2020 of the CAMS re-analysis (top panel) compared to the average for the period 2003–2019 (bottom panel). The CAMS re-analysis assimilated aerosol optical depth (AOD) retrievals from a Moderate Resolution Imaging Spectroradiometer (MODIS) and an Advanced Along-Track Scanning Radiometer (AATSR) and used Global Fire Assimilation System (GFAS) wildfire emissions.
Source: ECMWF/CAMS

[2] The troposphere is the lowest part of the atmosphere. It begins at the Earth's surface and reaches an altitude of 6–15 km, depending on the latitude.

a major factor behind advances in numerical weather prediction in recent decades (Bauer et al., 2015). The European Centre for Medium-Range Weather Forecasts (ECMWF) has extended this approach to forecasts around the globe for air quality, dust and fire plumes, stratospheric ozone and greenhouse gases as part of the Copernicus Atmosphere Monitoring Service, which the Centre implements on behalf of the European Union (Innes et al., 2019).

Computer-simulated fields corrected by observations are known as analyses corrected by observations are known analyses. Analyses are considered to be more accurate than model simulations, because systematic corrections based on observations from satellites, ground stations, aircraft and weather balloons ensure more comprehensive coverage than observational data sets alone ("maps with no gaps"). The analyses are used as initial conditions for the daily CAMS forecasts and for the retrospective study of atmospheric composition for understanding the spatial distribution, trends and variability of trace gases and aerosols.

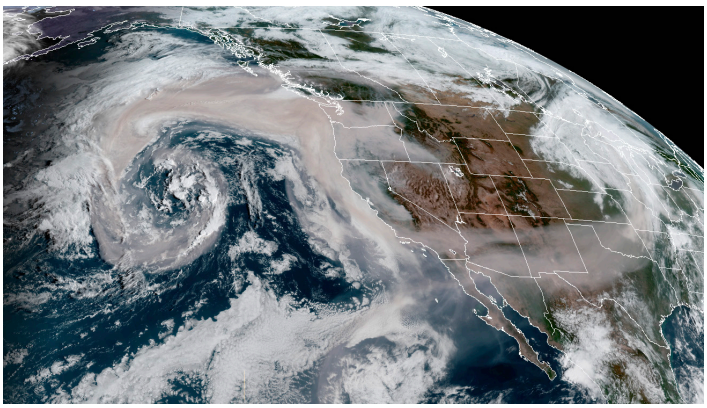

Figure 2. NOAA GOES-West satellite image taken on 12 September 2020, showing the entrainment of an unusually large and dense smoke plume from wildfires in the Pacific Northwest into a mid-latitude cyclone above the eastern North Pacific Ocean, and a second plume extending from the Desert Southwest into another mid-latitude cyclone above the upper Midwest. This image was generated by the Colorado State Satellite Loop Interactive Data Explorer in Real-time (SLIDER; http://rammb-slider.cira.colostate.edu, Micke, 2018).
Source: CSU/CIRA and NOAA/NESDIS

Interplay between climate, fires and air quality in 2020

To acquire a better understanding of how anthropogenic and natural emissions influence weather and air pollution, scientists at the NASA Global Modeling and Assimilation Office (https://gmao.gsfc.nasa.gov) combine a rich set of data sources with numerical models that represent physical and chemical processes occurring in the atmosphere. Models such as the Goddard Earth Observing System (GEOS) (Gelaro et al., 2017; Randles et al., 2017; Buchard et al., 2017; Keller et al., 2021; Molod et al., 2015) are powerful tools that can be used to complement sparse observational networks and create a comprehensive digital record of events such as the intense wildfire season in 2020.

The Global Modeling and Assimilation Office used satellite retrievals of fire locations and intensity to analyse wildfires in the extratropical regions of Eurasia and North America in 2020. The 2020 wildfire season was marked by extreme fires in Siberia and the western United States and uncharacteristically weak fire activity in Alaska and Canada, compared with the situation in previous decades. Comparisons with estimates of historical fire emissions (2003–2019) indicated that 2020 was an exceptional year in terms of total pyrogenic carbon released into the atmosphere by wildfires in Siberia and the western United States, with extremely dense and expansive smoke plumes visible from space (Figure 2). The Fire Weather Index(FWI; Wagner, 1987), a commonly used measure of fire intensity and potential, provided further insights into the anomalous fire season by quantifying how much influence key meteorological parameters such as temperature, wind, precipitation and humidity had on fire danger. The GEOS-based MERRA-2 analysis (Gelaro et al., 2017) was used to create a map that shows a substantially higher FWI in Siberia and the western United States, collocated with the observed fires (Figure 3).

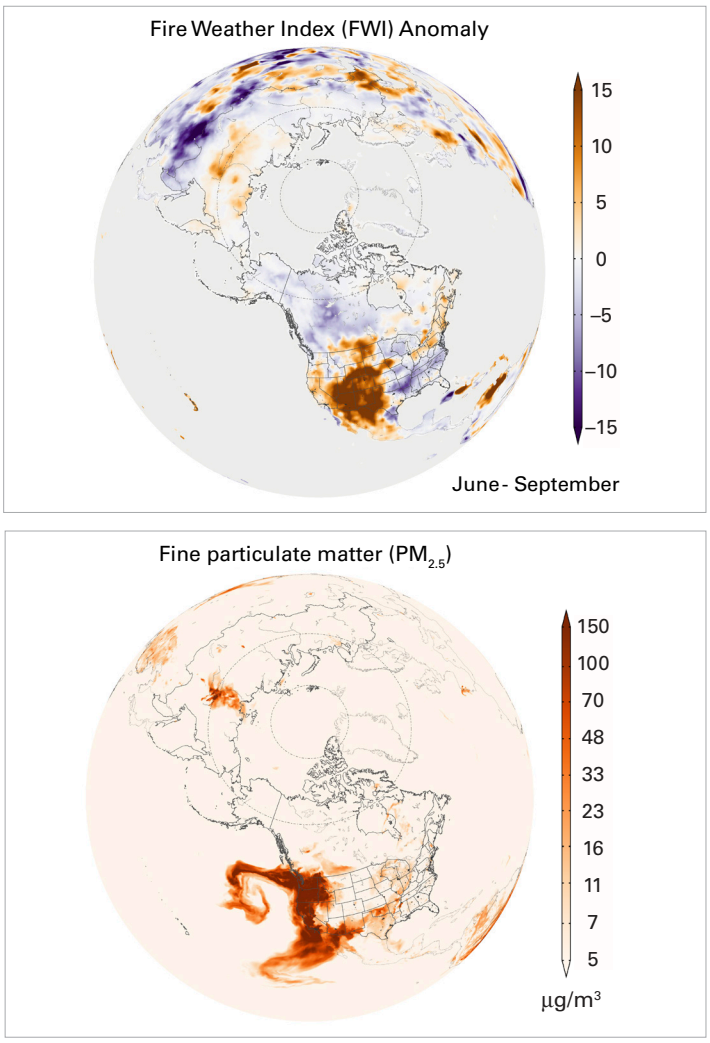

Figure 3. Top: Map of Fire Weather Index seasonal anomalies (2020 minus the mean of 2003–2019 for the period June–September). The higher the positive anomaly, the greater the increased fire potential; the lower the negative anomaly, the greater the reduced fire potential; bottom: Map of estimated fine particulate matter ($PM_{2.5}$) from fires on 13 September 2020, corresponding to the smoke plumes visible in Figure 2.
Source: NASA

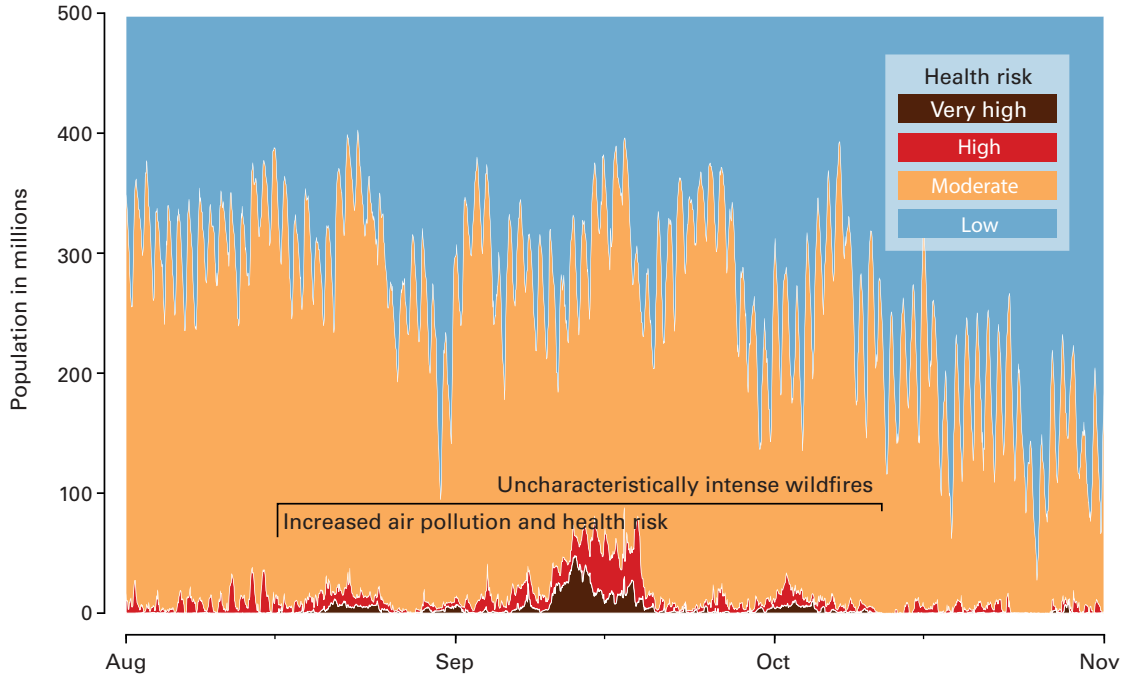

Figure 4. Air Quality and Health Index levels for people in North America during the 2020 wildfire season, based on air pollution caused by anthropogenic and natural sources.
Source: The Global Modeling and Assimilation Office, NASA

The strong relationship between negative departures from the FWI climatology and reduced potential for fires was also evident in Canada and Alaska. The behaviour of the fires in the major burning regions in the northern hemisphere extratropics can therefore be at least partly attributed to persistent weather patterns in the boreal summer of 2020, for example, a historic high-latitude heatwave in Siberia.

These conclusions are concerning because they may reflect a strengthening signal of changing climate on weather-induced mechanisms that alter fire behaviour and pollutant emissions on large scales. Several publications have pointed out that extreme heatwaves and dry spells are projected to be exacerbated by climate change (IPCC, 2021); one study concluded that the prolonged Siberian heatwave of 2020 would have been almost impossible without human influence (Ciavarella et al., 2021).

To assess the impact of the fires on outdoor air pollution across North America, the Global Modeling and Assimilation Office estimated how many people were exposed to varying levels of pollutants (Stieb et al., 2008). Using data from the multi-pollutant Air Quality and Health Index, the Office found that the number of people who likely experienced unhealthy levels of air pollution increased during the fire season and peaked in the second week of September, when most of the intense fires occurred in the western United States. For more than a week, 20–50 million people – mostly in the western United States but also in regions downwind – were classified as having a "High" or "Very High" health risk (Figure 4).

The impact of COVID-19 on air quality

Many governments around the world responded to the COVID-19 pandemic by restricting gatherings, closing schools and imposing lockdowns. These stay-at-home policies led to an unprecedented decrease in pollutant emissions. A study coordinated by the WMO/GAW examined the behaviour of key air-pollutant species during the COVID-19 pandemic (Sokhi et al., 2021).

Using a consistent approach, the study looked at the data from in situ ground-based air-quality observations from over 540 traffic, background and rural stations, in and around 63 cities from 25 countries located in seven geographical regions of the world. The data were used to analyse changes in air quality for the main pollutants, such as particulate matter ($PM_{2.5}$, PM_{10}, coarse fraction of PM) sulfur dioxide (SO_2), nitrogen oxides (NO_x), carbon monoxide (CO) and ozone (O_3), as well as for the total gaseous oxidant[3] ($OX = NO_2 + O_3$). The changes were examined for different lockdown stages, namely pre-lockdown, partial lockdown, full lockdown and two periods of relaxed restrictions between January and September 2020. The observational study investigated how changes in air quality were affected by emissions and regional and local meteorology in 2020 compared with the period 2015–2019.

During the various lockdown stages, emissions of air pollutants fell drastically across the globe due to travel

[3] An oxidant is a chemical substance that can oxidize other substances, which means it can accept the electrons of other substances.

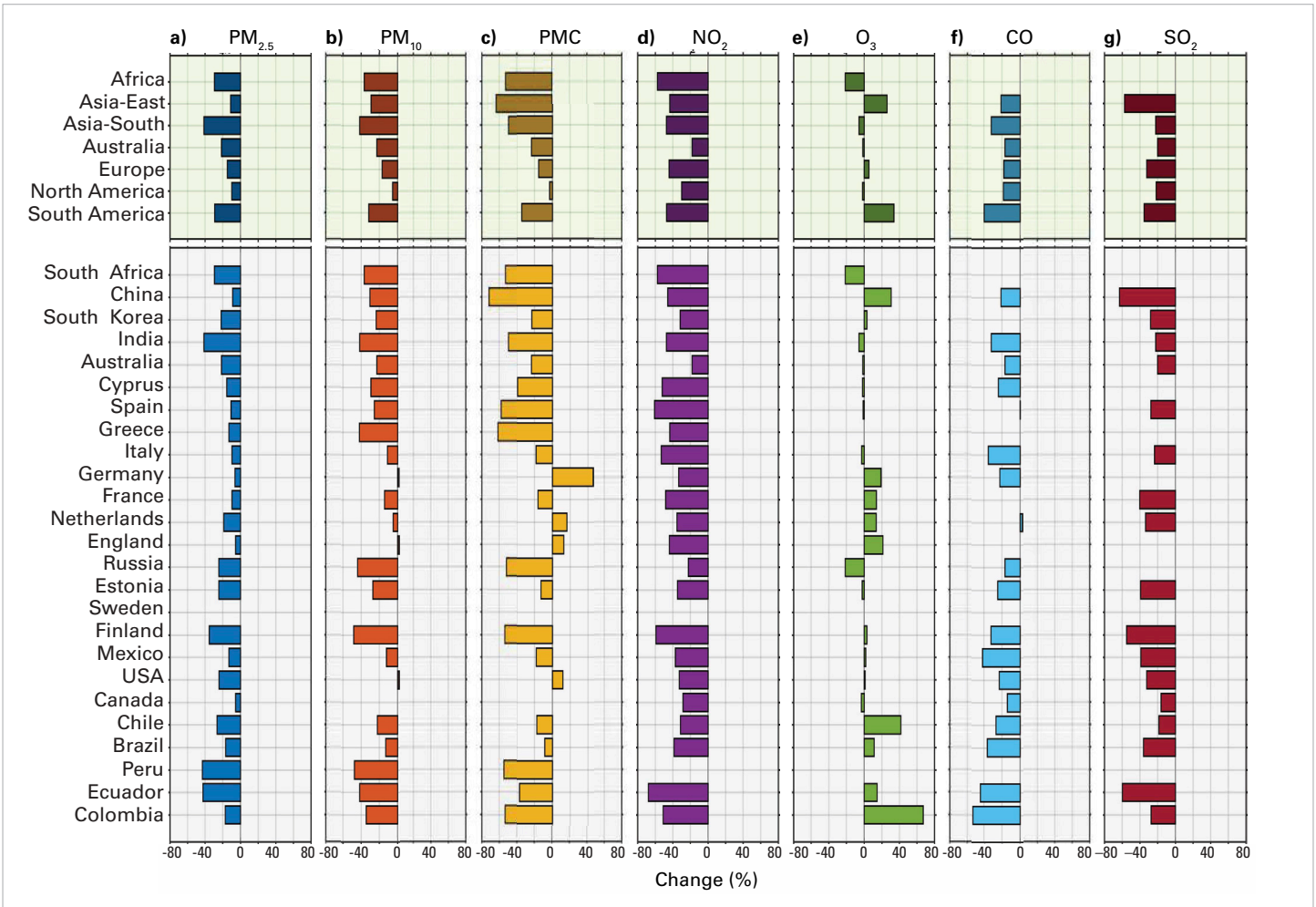

Figure 5. Continental/countrywide average changes in air pollution (in %) shown as bar plots for the full lockdown period for (a) $PM_{2.5}$, (b) PM_{10}, (c) PMC (coarse fraction of PM), (d) NO_2, (e) O_3, (f) CO and (g) SO_2.
Source: Modified from Sokhi et al., 2021

restrictions imposed to stem the spread of COVID-19. A positive correlation was observed between reductions in NO_2 and NO_x concentrations and a reduction in people's mobility for most cities. No clear indication was observed for other pollutants, which suggests that sources other than vehicle emissions also contributed substantially to the change in air quality.

Analysis showed (Figure 5) decreases of up to approximately 70% in mean NO_2 and 30%–40% in mean $PM_{2.5}$ concentrations during full lockdown in 2020 compared with the same periods in 2015–2019. $PM_{2.5}$, however, exhibited complex behaviour even within the same region, with increases in some Spanish cities, for instance, which were attributed mainly to the long-range transport of African dust and/or biomass burning. Some Chinese cities showed similar increases in $PM_{2.5}$ during the lockdown periods, probably due to secondary PM formation. Changes in ozone concentrations varied greatly among regions, ranging from no overall change to small increases (as was the case for Europe) and larger increases (+25% in East Asia and +30% in South America). Colombia showed the largest increase, at around 70%. Under certain polluted conditions, an increase in ozone might be expected, with decreases in its precursors, due to the complexities of ozone chemistry. Analysis of the total oxidant showed that primary NO_2 emissions at urban locations were greater than the O_3 production, whereas at background sites, OX was mostly driven by the regional contributions rather than local NO_2 and O_3 concentrations. SO_2 concentrations were between ~25% to 60% lower in 2020 than during 2015–2019 for all regions. CO levels were lower for all regions, with the largest decrease for South America, of up to approximately 40%.

This unplanned air-quality experiment can serve as a benchmark for policymakers to understand whether existing air-quality regulations would protect public health. While lockdowns had a clear impact on air quality in urban areas, the spatial and temporal extent of that impact, the specific role of meteorology and of episodic contributions (e.g. from dust, domestic and agricultural biomass burning and crop fertilization), and the cascade responses from indirect and non-linear effects are far from being fully understood. It is still necessary to better understand changes in how secondary pollutants chemically respond to emission changes under complex conditions and how socioeconomic drivers may affect future air quality. The implications for regional and global policies are also significant, as the Sokhi et al., 2021 study indicates that, in many parts of the world, $PM_{2.5}$ concentrations would be unlikely to meet World Health Organization guidelines, despite drastic reductions in mobility.

Low ozone values observed at GAW background stations

Figure 6 shows the long-term ozone concentration variability at three very remote locations. North of the Arctic Circle, the Barrow Atmospheric Baseline Observatory on the northern shore of Alaska, shows ozone concentration has increased by 11% since records began in 1973. Ozone concentration in the tropical North Pacific Ocean has increased by 17% since 1973, as observed at Mauna Loa Observatory, located at 3 400 m above sea level on the island of Hawaii. Historical data from Mauna Loa show that ozone concentration has increased by approximately 50% since the late 1950s. At the South Pole Observatory, as far away from human activity as possible, ozone concentration has increased by 6% since 1975. All three sites show a strong seasonal cycle, but the timing of the annual maximum varies due to differences in photochemistry and the weather patterns that transport ozone to these remote sites (Cooper et al., 2020).

Figure 6 also shows the long-term changes in ozone concentration near the Alpine summit of Zugspitze in southern Germany (2 800 m elevation). Depending on highly variable weather patterns, these ozone values can be representative of air that originates within the polluted boundary layer[4] of Europe or air that originates beyond western Europe. Ozone concentration increased during the period from when records began (1978) until the late 1990s. Since 2000, ozone concentration has changed relatively little, although levels have decreased slightly during the warm months of May-September, when Zugspitze is most frequently affected by regional European pollution (Cooper et al., 2020).

[4] The planetary boundary layer is the lowest part of the troposphere and strongly influenced by surface turbulence.

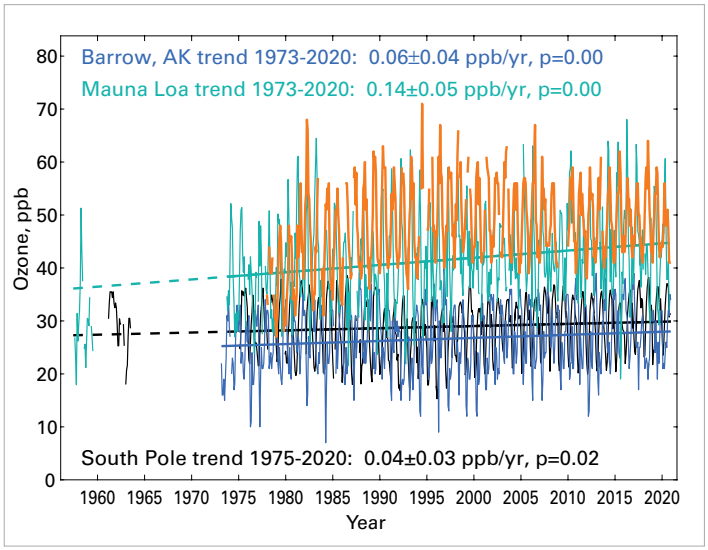

Figure 6. Monthly ozone values at three GAW global background monitoring sites: Barrow Atmospheric Baseline Observatory, Alaska (11 m elevation); Mauna Loa Observatory, Hawaii (3 397 m elevation), and the South Pole Observatory (2 837 m elevation). Also shown are the monthly ozone values near the summit of Zugspitze (2 800 m elevation) on the southern border of Germany (orange).
ppb (parts per billion) is the number of molecules of the gas per billion (10^9) molecules of dry air
Source: Modified from Cooper et al., 2020.

Monte Cimone – the highest mountain in the northern Apennines of Italy – has a WMO/GAW station at its summit. A recent study has shown that ozone levels at Monte Cimone were unusually low in the boreal spring and summer of 2020, likely due to reduced European emissions during the COVID-19 economic downturn (Cristofanelli et al., 2021). Similar reductions are seen at Zugspitze, 350 km to the north (Figure 7). Low ozone values in May, June and July were also observed at the hilltop site of Hohenpeissenberg, Germany, but the

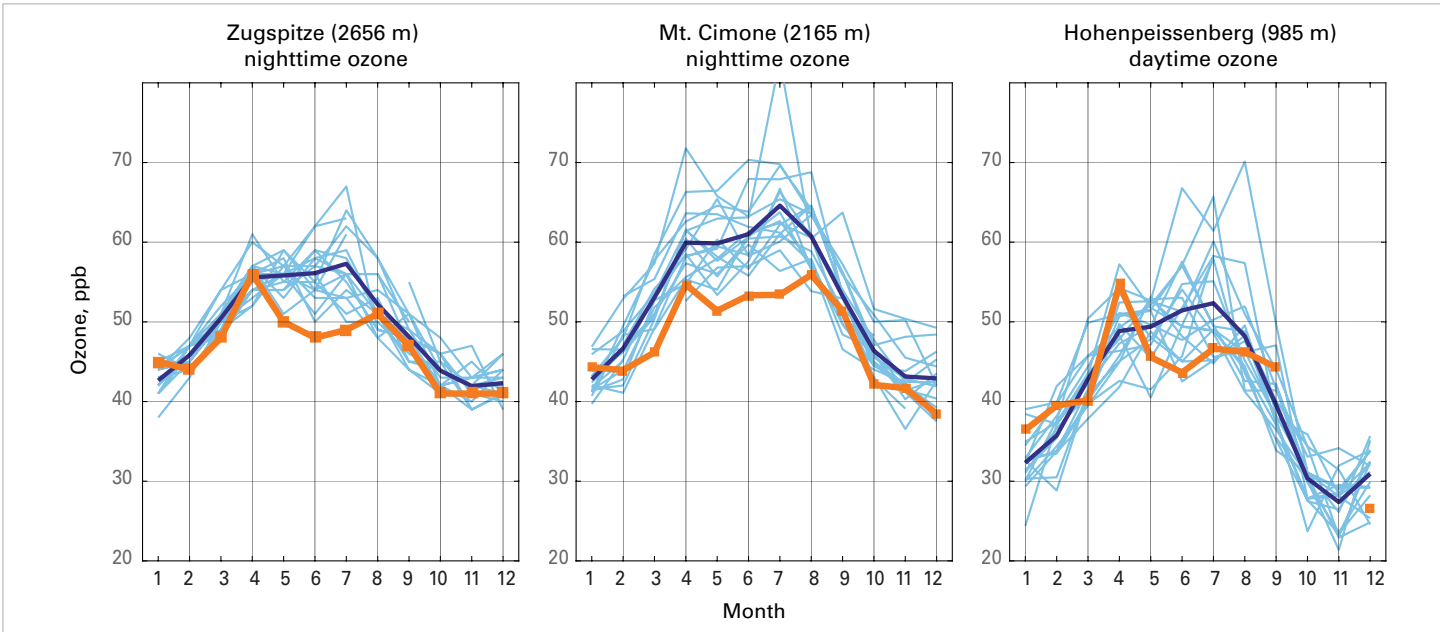

Figure 7. Left: Night-time monthly mean ozone at Zugspitze, Germany for 2020 (orange) compared with individual years from 2002 to 2019 (light blue) and the mean of the years 2002–2019 (dark blue). Centre: Night-time monthly mean ozone at Monte Cimone, Italy. Right: Daytime mean ozone at Hohenpeissenberg, Germany.
Source: Drawn by Owen Cooper

reductions relative to multi-year average were not as low as those observed at Zugspitze, 40 km to the south. The spring and summer ozone reductions at Monte Cimone and Zugspitze are highly unusual and are lower than anything observed over the past two decades. These reductions are even greater than those observed in the free troposphere across the northern hemisphere mid-latitudes by weather balloons, lidar (laser instrument) and commercial aircraft in 2020 (Steinbrecht et al., 2021; Clark et al., 2021), indicating that the COVID-19 economic downturn had a broad impact on ozone production across Europe.

Global mortality estimates for ambient and household air pollution

The Global Burden of Disease (GBD) initiative provides regular updates (two-year cycle) on premature death and disability from 369 diseases and injuries in 204 countries and territories (Murray et al., 2020), from 1990 to the present, including environmental health threats such as poor air quality due to ambient (outdoor) ozone pollution, ambient particulate matter (in particular $PM_{2.5}$) and household (indoor) particulate matter (http://www.healthdata.org/gbd/about).

GBD quantifies global-scale exposure to ambient ozone pollution by combining observations from thousands of surface-air-quality monitoring stations worldwide with output from atmospheric chemistry models (Schultz et al., 2017; Chang et al., 2019; DeLang et al., 2021). Similarly, exposure to $PM_{2.5}$ is based on observations at thousands of monitoring stations worldwide combined with global satellite observations of column particulate matter and output from an atmospheric chemistry model (van Donkelaar et al., 2017). Global exposure maps of ambient ozone and ambient $PM_{2.5}$ were produced for the years 1990–2019, which allowed GBD scientists to estimate annual mortality due to long-term exposure (Murray et al., 2020).

Figure 8 shows ambient air-pollution mortality estimates from the latest GBD assessment (Murray et al., 2020). Global mortality due to ambient air pollution is dominated by particulate matter with 4.1 million deaths in 2019,

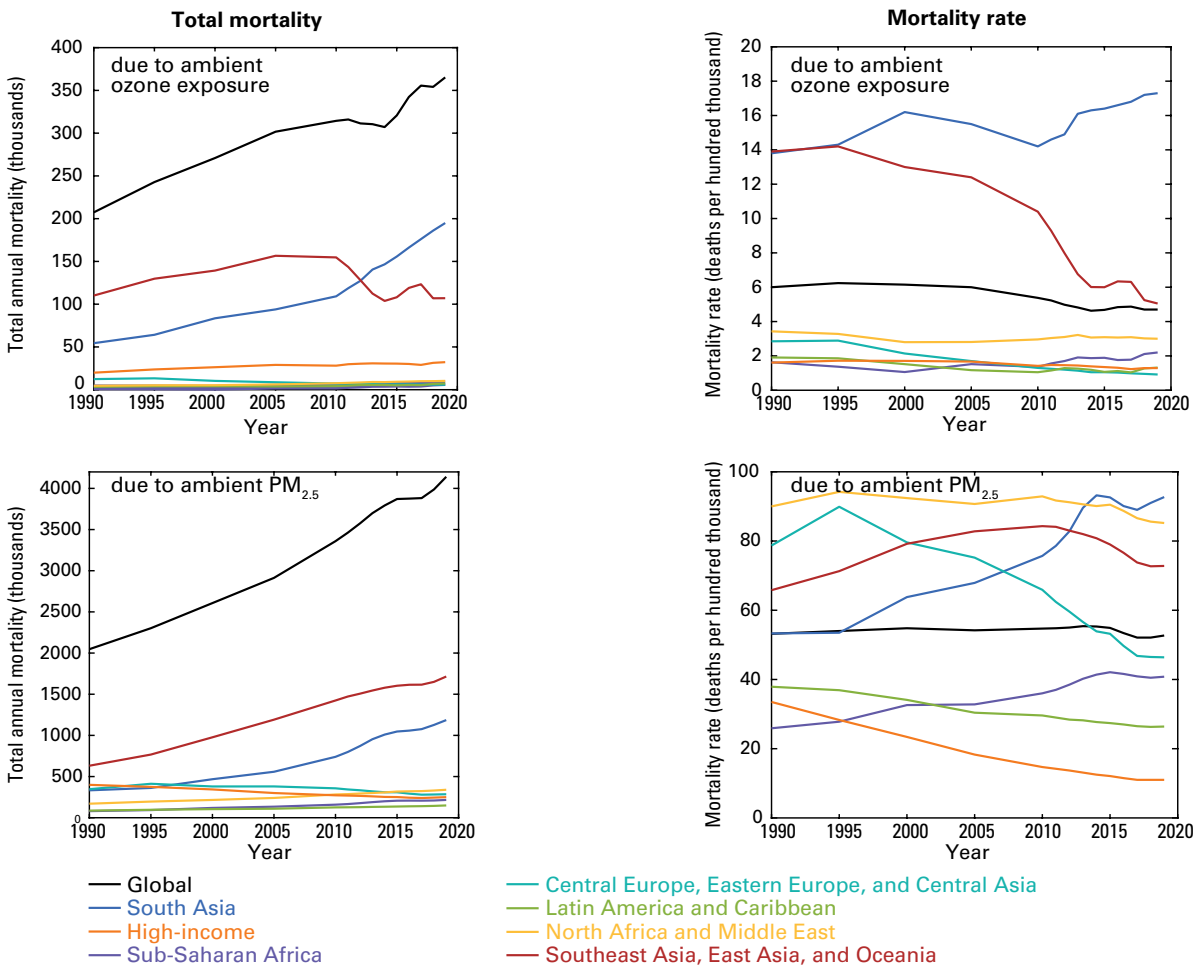

Figure 8. Global Burden of Disease 2019 mortality estimates. Note that the total mortality values along the $PM_{2.5}$ y-axis are a factor of 10 greater than the values along the ozone y-axis, and the mortality rate values along the $PM_{2.5}$ y-axis are a factor of 5 greater than the values along the ozone y-axis. Data are displayed for the seven super-regions created by GBD and based on two criteria: epidemiological similarity and geographic closeness. The "High-income" region includes the United States, Canada, Chile, Argentina, Uruguay, Western Europe, Israel, Australia, New Zealand, Japan and Republic of Korea. A map of the super-regions is available at http://www.healthdata.org/gbd/faq.
Source: Murray et al., 2020.

compared with 365 000 deaths due to ambient ozone exposure. These estimates are not exact and the uncertainty (95% uncertainty interval) on these values is ±20% for ambient particulate matter, and ±50% for ambient ozone (Health Effects Institute, 2020). In total, global mortality increased from 2.3 million in 1990 (91% due to particulate matter, 9% due to ozone) to 4.5 million in 2019 (92% due to particulate matter, 8% due to ozone). Regionally, present-day total mortality is greatest in the super-region of Southeast Asia, East Asia and Oceania (1.8 million total deaths; 94% due to particulate matter, 6% due to ozone), followed by the South Asia super-region (1.4 million total deaths; 86% due to particulate matter, 14% due to ozone). The global mortality rate (deaths per 100 000) due to ambient ozone pollution has decreased by 13% since 2010, and the global mortality rate due to ambient particulate matter has decreased by 4%.

Another major cause of premature mortality is household particulate matter, which is caused by the burning of solid and liquid fuels for cooking and home heating. GBD assesses mortality due to the burning of solid fuel for cooking and estimates that there were 2.3 million (uncertainty of ±30%) premature deaths in 2019 (Health Effects Institute, 2020). Therefore, the GBD estimate of total global mortality due to ambient and household air pollution for the year 2019 is 6.8 million, of which 34% is due to cooking-related household particulate matter. The great majority of deaths associated with household particulate matter occur in the super-regions of South Asia, Sub-Saharan Africa, and Southeast Asia, East Asia and Oceania. While total mortality due to household particulate matter has steadily decreased in these regions since 2010, mortality rates remain high, especially in sub-Saharan Africa, where the mortality rate due to household particulate matter is roughly three times the rate due to ambient particulate matter. An in-depth analysis of global mortality due to ambient and household air pollution can be found in the State of Global Air 2020 (Health Effects Institute, 2020).

Conclusions

In conclusion, this issue of the *WMO Air Quality and Climate Bulletin* highlights the critical role that observations play in monitoring the state of the atmosphere. Long-term, consistent measurements enable the community to understand how conditions have changed relative to the past and empower air quality and climate models to improve simulations of the atmosphere. There is still room for improvement – model predictions will always be somewhat uncertain – but in times of rapid shifts in human activity (as was the case in 2020), filling observational gaps for key species will greatly improve our ability to model atmospheric changes as they occur. The WMO Global Atmosphere Watch (WMO/GAW, 2014; Schultz et al., 2015) supports atmospheric composition measurements, analysis and research, including the linkages between air quality and climate. Many pollutants (reactive gases and aerosols) are part of the extensive measurement programmes carried out at GAW stations around the world. These data provide a unique record of Earth's changing atmospheric chemical composition. GAW stations provide valuable data for assessing global ozone and aerosol trends (Tarasick et al., 2019, Collaud Coen et al., 2020), conducting climate-change research (Hartmann et al., 2013, Laj et al., 2020), evaluating global and regional climate-chemistry models (Mortier et al., 2020, Gliß et al., 2021) and quantifying the global impact of ozone on human health (Chang et al., 2019; DeLang et al., 2021).

References

Bauer, P.; Thorpe, A.; Brunet, G. The Quiet Revolution of Numerical Weather Prediction. *Nature* **2015**, 525 (7567), 47–55. https://doi.org/10.1038/nature14956.

Buchard, V.; Randles, C. A.; Silva, A. M. da et al. The MERRA-2 Aerosol Reanalysis, 1980 Onward. Part II: Evaluation and Case Studies. *Journal of Climate* **2017**, 30 (17), 6851–6872. https://doi.org/10.1175/JCLI-D-16-0613.1.

Chakraborty, S.; Guan, B.; Waliser, D. E. et al. Extending the Atmospheric River Concept to Aerosols: Climate and Air Quality Impacts. *Geophysical Research Letters* **2021**, 48 (9), e2020GL091827. https://doi.org/10.1029/2020GL091827.

Chang, K.-L.; Cooper, O. R.; West, J. J. et al. A New Method (M3Fusion v1) for Combining Observations and Multiple Model Output for an Improved Estimate of the Global Surface Ozone Distribution. Geoscientific Model Development **2019**, 12 (3), 955–978. https://doi.org/10.5194/gmd-12-955-2019.

Ciavarella, A.; Cotterill, D.; Stott, P. et al. Prolonged Siberian Heat of 2020 Almost Impossible without Human Influence. *Climatic Change* **2021**, 166 (1), 9. https://doi.org/10.1007/s10584-021-03052-w.

Clark, H.; Bennouna, Y.; Tsivlidou, M. et al. The Effects of the COVID-19 Lockdowns on the Composition of the Troposphere as Seen by IAGOS. *Atmospheric Chemistry and Physics Discussions* **2021**, 1–33. https://doi.org/10.5194/acp-2021-479.

Collaud Coen, M.; Andrews, E.; Alastuey, A. et al. Multidecadal Trend Analysis of in Situ Aerosol Radiative Properties around the World. Atmospheric *Chemistry and Physics* **2020**, 20 (14), 8867–8908. https://doi.org/10.5194/acp-20-8867-2020.

Cooper, O. R.; Schultz, M. G.; Schröder, S. et al. Multi-Decadal Surface Ozone Trends at Globally Distributed Remote Locations. *Elementa: Science of the Anthropocene* **2020**, 8 (23). https://doi.org/10.1525/elementa.420.

Cristofanelli, P.; Arduni, J.; Serva, F. et al. Negative Ozone Anomalies at a High Mountain Site in Northern Italy during 2020: A Possible Role of COVID-19 Lockdowns? *Environ. Res. Lett.* **2021**, 16 (7), 074029. https://doi.org/10.1088/1748-9326/ac0b6a.

DeLang, M. N.; Becker, J. S.; Chang, K.-L. et al. Mapping Yearly Fine Resolution Global Surface Ozone through the Bayesian Maximum Entropy Data Fusion of Observations and Model Output for 1990–2017. *Environ. Sci. Technol.* **2021**, 55 (8), 4389–4398. https://doi.org/10.1021/acs.est.0c07742.

Fasullo, J. T.; Rosenbloom, N.; Buchholz, R. R. et al. Coupled Climate Responses to Recent Australian Wildfire and COVID-19 Emissions Anomalies Estimated in CESM2. *Geophysical Research Letters* **2021**, 48 (15), e2021GL093841. https://doi.org/10.1029/2021GL093841.

Fiore, A. M.; Naik, V.; Spracklen, D. V. et al. Global Air Quality and Climate. *Chem. Soc. Rev.* **2012**, 41 (19), 6663–6683. https://doi.org/10.1039/C2CS35095E.

Gelaro, R.; McCarty, W.; Suárez, M. J. et al. The Modern-Era Retrospective Analysis for Research and Applications, Version 2 (MERRA-2). *Journal of Climate* **2017**, 30 (14), 5419–5454. https://doi.org/10.1175/JCLI-D-16-0758.1.

Gkatzelis, G. I.; Gilman, J. B.; Brown, S. S. et al. The Global Impacts of COVID-19 Lockdowns on Urban Air Pollution: A Critical Review and Recommendations. *Elementa: Science of the Anthropocene* **2021**, 9 (1). https://doi.org/10.1525/elementa.2021.00176.

Gliß, J.; Mortier, A.; Schulz, M. et al. AeroCom Phase III Multi-Model Evaluation of the Aerosol Life Cycle and Optical Properties Using Ground- and Space-Based Remote Sensing as Well as Surface in Situ Observations. *Atmospheric Chemistry and Physics* **2021**, 21 (1), 87–128. https://doi.org/10.5194/acp-21-87-2021.

Hartmann, D.L., Klein Tank, A.M.G., Rusticucci, M. et al. Chapter 2. *Observations: Atmosphere and Surface*. In:*Climate Change 2013: The Physical Science Basis. Contribution of Working Group I to the Fifth Assessment Report of the Intergovernmental Panel on Climate Change*, Stocker, T.F. et al., (eds.), Cambridge University Press, Cambridge, United Kingdom and New York, 2013. https://www.ipcc.ch/site/assets/uploads/2017/09/WG1AR5_Chapter02_FINAL.pdf.

Health Effects Institute. *State of Global Air 2020*. Special Report. 2020. Boston, MA: Health Effects Institute. https://www.stateofglobalair.org/sites/default/files/documents/2020-10/soga-2020-report-10-26_0.pdf.

Inness, A.; Ades, M.; Agustí-Panareda, A.; Barré, J. et al. The CAMS Reanalysis of Atmospheric Composition. *Atmospheric Chemistry and Physics* **2019**, 19 (6), 3515–3556. https://doi.org/10.5194/acp-19-3515-2019.

IPCC. *Climate Change 2021: The Physical Science Basis. Contribution of Working Group I to the Sixth Assessment Report of the Intergovernmental Panel on Climate Change*. 2021. (Masson-Delmotte, V. et al., Eds.). https://www.ipcc.ch/report/sixth-assessment-report-working-group-i/.

Kaiser, J. W.; Heil, A.; Andreae, M. O. et al. Biomass Burning Emissions Estimated with a Global Fire Assimilation System Based on Observed Fire Radiative Power. *Biogeosciences* **2012**, 9 (1), 527–554. https://doi.org/10.5194/bg-9-527-2012.

Keller, C. A.; Knowland, K. E.; Duncan, B. N. et al. Description of the NASA GEOS Composition Forecast Modeling System GEOS-CF v1.0. *Journal of Advances in Modeling Earth Systems* **2021**, 13 (4), e2020MS002413. https://doi.org/10.1029/2020MS002413.

Laj, P.; Bigi, A.; Rose, C. et al. A Global Analysis of Climate-Relevant Aerosol Properties Retrieved from the Network of Global Atmosphere Watch

(GAW) near-Surface Observatories. *Atmospheric Measurement Techniques* **2020**, 13 (8), 4353–4392. https://doi.org/10.5194/amt-13-4353-2020.

Micke, K. Every Pixel of GOES-17 Imagery at Your Fingertips. *Bulletin of the American Meteorological Society* **2018**, 99 (11), 2217–2219. https://doi.org/10.1175/BAMS-D-17-0272.1.

Molod, A.; Takacs, L.; Suarez, M. et al. Development of the GEOS-5 Atmospheric General Circulation Model: Evolution from MERRA to MERRA2. *Geoscientific Model Development* **2015**, 8 (5), 1339–1356. https://doi.org/10.5194/gmd-8-1339-2015.

Mortier, A.; Gliß, J.; Schulz, M. et al. Evaluation of Climate Model Aerosol Trends with Ground-Based Observations over the Last 2 Decades – an AeroCom and CMIP6 Analysis. *Atmospheric Chemistry and Physics* **2020**, 20 (21), 13355–13378. https://doi.org/10.5194/acp-20-13355-2020.

Murray, C. J. L.; Aravkin, A. Y.; Zheng, P. et al. Global Burden of 87 Risk Factors in 204 Countries and Territories, 1990–2019: A Systematic Analysis for the Global Burden of Disease Study 2019. *The Lancet* **2020**, 396 (10258), 1223–1249. https://doi.org/10.1016/S0140-6736(20)30752-2.

Pye, H. O. T.; Liao, H.; Wu, S. et al. Effect of Changes in Climate and Emissions on Future Sulfate-Nitrate-Ammonium Aerosol Levels in the United States. *Journal of Geophysical Research: Atmospheres* **2009**, 114 (D1). https://doi.org/10.1029/2008JD010701.

Randles, C. A.; Silva, A. M. da; Buchard, V. et al. The MERRA-2 Aerosol Reanalysis, 1980 Onward. Part I: System Description and Data Assimilation Evaluation. *Journal of Climate* **2017**, 30 (17), 6823–6850. https://doi.org/10.1175/JCLI-D-16-0609.1.

Schultz, M. G.; Akimoto, H.; Bottenheim, J. et al. The Global Atmosphere Watch Reactive Gases Measurement Network. *Elementa: Science of the Anthropocene* **2015**, 3 (000067). https://doi.org/10.12952/journal.elementa.000067.

Schultz, M. G.; Schröder, S.; Lyapina, O. et al. Tropospheric Ozone Assessment Report: Database and Metrics Data of Global Surface Ozone Observations. *Elementa: Science of the Anthropocene* **2017**, 5 (58). https://doi.org/10.1525/elementa.244.

Sokhi, R. S.; Singh, V.; Querol, X. et al. A Global Observational Analysis to Understand Changes in Air Quality during Exceptionally Low Anthropogenic Emission Conditions. *Environment International* **2021**, 157, 106818. https://doi.org/10.1016/j.envint.2021.106818.

Steinbrecht, W.; Kubistin, D.; Plass-Dülmer, C. et al. COVID-19 Crisis Reduces Free Tropospheric Ozone Across the Northern Hemisphere. *Geophysical Research Letters* **2021**, 48 (5), e2020GL091987. https://doi.org/10.1029/2020GL091987.

Stieb, D. M.; Burnett, R. T.; Smith-Doiron, M. et al. A New Multipollutant, No-Threshold Air Quality Health Index Based on Short-Term Associations Observed in Daily Time-Series Analyses. *Journal of the Air & Waste Management Association* **2008**, 58 (3), 435–450. https://doi.org/10.3155/1047-3289.58.3.435.

Tarasick, D.; Galbally, I. E.; Cooper, O. R. et al. Tropospheric Ozone Assessment Report: Tropospheric Ozone from 1877 to 2016, Observed Levels, Trends and Uncertainties. *Elementa: Science of the Anthropocene* **2019**, 7 (39). https://doi.org/10.1525/elementa.376.

van Donkelaar, A.; Martin, R. V.; Brauer, M. et al. Global Estimates of Fine Particulate Matter Using a Combined Geophysical-Statistical Method with Information from Satellites, Models, and Monitors. *Environ. Sci. Technol.* **2016**, 50 (7), 3762–3772. https://doi.org/10.1021/acs.est.5b05833.

Wagner, C. E. V. *Development and Structure of the Canadian Forest Fire Weather Index System*; Forestry technical report; Canada Communication Group Publ: Ottawa, 1987.

West, J. J.; Smith, S. J.; Silva, R. A. et al. Co-Benefits of Mitigating Global Greenhouse Gas Emissions for Future Air Quality and Human Health. *Nature Clim Change* **2013**, 3 (10), 885–889. https://doi.org/10.1038/nclimate2009.

World Meteorological Organization (WMO), *WMO Aerosol Bulletin*. No. 4, 2021. https://library.wmo.int/index.php?lvl=notice_display&id=21886#.YS421tMzZGw.

World Meteorological Organization (WMO), *WMO Airborne Dust Bulletin*. No. 5, 2021. https://library.wmo.int/index.php?lvl=notice_display&id=19826#.YS42btMzZGw.

WMO/GAW. *The Global Atmosphere Watch Programme: 25 Years of Global Coordinated Atmospheric Composition Observations and Analyses*. WMO Report. WMO-No. 1143. https://library.wmo.int/doc_num.php?explnum_id=7886.

Acknowledgements and links

Data for aerosols and reactive gases collected within the GAW Programme with support from WMO Members and contributing networks are available from the World Data Centre for Aerosols and Reactive Gases, which is supported by the Norsk Institutt for Luftforskning, Norway. Carbon monoxide data are available from the World Data Centre for Greenhouse Gases, which is supported by the Japan Meteorological Agency. GAW stations are described in the GAW Station Information System (https://gawsis.meteoswiss.ch/), which is supported by MeteoSwiss.

All data from the Copernicus Atmosphere Monitoring Service are freely available from the Atmosphere Data Store: https://ads.atmosphere.copernicus.eu.

This Bulletin contains contributions from the WMO/GAW Scientific Advisory Group on Aerosols, the Scientific Advisory Group on Applications, the Scientific Advisory Group for GAW Urban Research Meteorology and Environment, the Scientific Advisory Group for Reactive Gases and the Steering Committee of Global Air Quality Forecasting and Information System.

GBD mortality estimates due to ambient and household air pollution can be downloaded from https://www.stateofglobalair.org/.

Editorial Board

Owen. R. Cooper (CIRES University of Colorado Boulder/NOAA CSL, United States of America), Ranjeet. S. Sokhi (University of Hertfordshire, United Kingdom of Great Britain and Northern Ireland), Julie. M. Nicely (University of Maryland and NASA, United States), Greg Carmichael (University of Iowa, United States), Anton Darmenov (NASA, United States), Paolo Laj (Université Grenoble Alpes, France, and University of Helsinki, Finland) and John Liggio (Environment and Climate Change Canada).

All authors in alphabetic order:

Maria de Fatima Andrade (Universidade de São Paulo, Brazil), Greg Carmichael (University of Iowa, United States), Owen R.Cooper (CIRES University of Colorado Boulder/NOAA CSL, United States), Cedric Couret (German Environment Agency (UBA), Germany), Paolo Cristofanelli (Institute of Atmospheric Sciences and Climate (CNR-ISAC), Italy), Anton Darmenov (NASA, United States), Sandro Finardi (ARIANET, Italy), Johannes Flemming (ECMWF), Rebecca M. Garland (Council for Scientific and Industrial Research, North-West University and University of Pretoria, South Africa), Shaofei Kong (China University of Geosciences, China), Dagmar Kubistin (Deutscher Wetterdienst, Germany), Paolo Laj (Université Grenoble Alpes, France, and University of Helsinki, Finland), John Liggio (Environment and Climate Change Canada, Canada), Jordi Massagué (Institute of Environmental Assessment and Water Research, Spanish Research Council and Universitat Politècnica de Catalunya, Spain), Julie M. Nicely (University of Maryland and NASA, United States), Radenko Pavlovic (Environment and Climate Change Canada, Canada), Irina Petropavlovskikh (CIRES University of Colorado Boulder/NOAA GML , United States), Vincent-Henri Peuch (ECMWF), Xavier Querol (Institute of Environmental Assessment and Water Research, Spanish Research Council, Spain), Samuel Rémy (HYGEOS), Vikas Singh (National Atmospheric Research Laboratory, India), Ranjeet S. Sokhi (University of Hertfordshire, United Kingdom), Admir Créso Targino (Federal University of Technology, Brazil).

Contacts

World Meteorological Organization

Atmospheric Environment Research Division
Science and Innovation Department, Geneva, Switzerland
Email: gaw@wmo.int
Website: https://community.wmo.int/activity-areas/gaw

World Data Centre for Greenhouse Gases

Japan Meteorological Agency, Tokyo
Email: wdcgg@met.kishou.go.jp
Website: https://gaw.kishou.go.jp/

World Data Centre for Reactive Gases & World Data Centre for Aerosols

Norwegian Institute for Air Research (NILU), Kjeller, Norway
Email: kt@nilu.no
Website: https://www.gaw-wdcrg.org/
https://www.gaw-wdca.org/

JN 211148